

PFC/JA-83-32R

STEADY STATE SOLUTION OF A TWO-DIMENSIONAL FOKKER-
PLANCK EQUATION WITH STRONG QUASILINEAR DIFFUSION
FOR LOWER-HYBRID CURRENT DRIVE*

by

V. B. Krapchev, D. W. Hewett⁺ and A. Bers

Revised May 1984

* This work was supported in part by DOE Contract No. DE-AC02-78ET-51013 and in part by NSF Grant ECS 82-13430. This is the revised version of Report PFC/JA-83-32 issued in August 1983, and replaces it.

⁺ Now at LLNL, Livermore, California.

STEADY STATE SOLUTION OF A TWO-DIMENSIONAL FOKKER-PLANCK EQUATION WITH STRONG QUASILINEAR DIFFUSION FOR LOWER-HYBRID CURRENT DRIVE*

V. B. Krapchev, D. W. Hewett** and A. Bers

*Plasma Fusion Center
Massachusetts Institute of Technology
Cambridge, Massachusetts 02139*

Abstract

We solve analytically and numerically the two-dimensional Fokker-Planck equation with strong quasilinear diffusion on the tail of the electron distribution function. The quasilinear diffusion is taken to be parallel to the confining magnetic field of the plasma, as is appropriate for lower-hybrid current drive. The RF fields that produce this quasilinear diffusion are assumed to be imposed by external sources. We find that an appreciable broadening of the resonant plateau in the direction perpendicular to the toroidal magnetic field leads to more particles carrying the current. As a result both the current (J) and the power dissipated (P_d) are substantially enhanced, compared with the predictions of one-dimensional theory. The figure of merit J/P_d is three times larger than the one found from the one-dimensional theory.

*This work was supported in part by DOE Contract No. DE-AC02-78ET-51013 and in part by NSF Grant ECS 82-13430.

**Now at LLNL, Livermore, California

I. Introduction

Steady state tokamak operation requires that the toroidal plasma current be driven continuously. An attractive approach is to use radio frequency (RF) waves. In many cases RF waves use only a small fraction of the fusion power output to maintain the confining current. It has been shown that the high phase velocity lower hybrid (LH) waves are particularly promising.¹ In that case the current is carried by electrons traveling in phase with the waves at several thermal velocities (v_t), and they collide relatively infrequently. These electrons form a plateau on the tail of the electron distribution function. The number of particles in that plateau and its slope determine the current density (J) and the power dissipated (P_d). The figure of merit is the ratio J/P_d . Both a one-dimensional (1D) theory¹ and a two-dimensional (2D) numerical investigation² have shown nearly identical values for J and their results for J/P_d differ by a multiplicative factor of 2.5, the 2D numerical study predicting the higher value. The 2D numerical study also noted that in the $v_{||}$ range of the applied RF spectrum the distribution function in v_{\perp} was broader than the Maxwellian in the absence of RF, but this effect was not investigated in detail. The 1D theory assumed that the perpendicular distribution function remained a Maxwellian and at the same temperature as in the absence of RF.

Recent LH current drive experiments have generated an appreciable current.^{3,4} The experiments agree roughly with the theory on the figure of merit scheme, J/P_d . However, the current itself differs significantly from theoretical values based upon Refs. 1 and 2 if the excited waves are assumed to have a spectrum as may be calculated⁵ from the waveguide array excitation at the plasma edge. Based upon the results of Refs. 1 and 2, attempts have been made to explain this discrepancy by an upshift in the parallel refractive index as the fields propagate from the plasma edge to the center. Various mechanisms can be invoked to give rise to such an upshift: toroidal effects in ray propagation⁶; scattering from density fluctuations⁷; nonlinear effects in coupling⁸ and propagation^{9,10}; and the generation of unstable spectra¹¹. All of these mechanisms remain unconfirmed, and, at best, difficult to confirm, experimentally. Furthermore, the experiments of Refs. 3 and 4 show a very large enhancement of the perpendicular distribution function.^{12,13} In view of these experimental results a deeper understanding of 2D velocity-space effects in steady-state current drive is required before invoking an upshift in the parallel wavenumbers of the applied RF fields.

In this paper we present results of a new numerical integration of the 2D Fokker Planck equation supplemented by parallel quasilinear diffusion, together with supporting 2D analytical work that gives a more complete picture of LH current drive. As in the past, we focus our study on the steady state regime in which current generation is achieved with strong quasilinear diffusion on a time scale which is short

compared to the heating of the bulk; thus the temperature evolution of the bulk distribution function is ignored. In contrast with the results of Ref. 2, we find that for a given RF spectrum the 2D solutions give a much larger current than would be calculated from the 1D theory. Our analytical work on the 2D problem predicts the numerically observed enhancement of the figure of merit over that given by 1D theory. Furthermore, by introducing an approximate treatment of the boundary conditions at the edges of the spectrum, we are able to arrive at approximate solutions of the 2D problem which give the current density and perpendicular temperature in the velocity regime of the applied spectrum.

In section II we describe our numerical integration of the 2D velocity space equation for tail electrons and compare our results with those of Ref. 2. In section III we give an approximate analytic treatment of the 2D problem and show that this formulation is supported by the numerical integration results obtained in section II. Section IV summarizes our findings and their importance for future work aimed at understanding experiments in LH current drive.

II. Model Equations and Numerical Integration Results

In the present study we solve numerically and analytically the 2D Fokker-Planck equation with parallel quasilinear diffusion as is pertinent for tail electrons in the presence of LH fields for RF current drive. For these electrons, the Landau collisional term is linearized. This is justified because the RF diffusion is taken to affect mostly the particles on the tail of the distribution function. We retain the collisions between tail and bulk particles, but neglect those between tail and tail particles as insignificant. The collisional term can be simplified further by noting that $m_e/m_i \ll 1$ and $T_e/T_i \sim O(1)$ where $m_e(m_i)$ is the mass of electrons (ions) and $T_e(T_i)$ are their respective temperatures. Thus the ions are much slower than the electrons and their distribution function can be taken as a δ -function in the integrand of the collisional term. The resulting equation is the one treated in Ref. 2:

$$\frac{\partial f}{\partial \tau} = \frac{\partial}{\partial v_{\parallel}} D(v_{\parallel}) \frac{\partial f}{\partial v_{\parallel}} + \frac{1}{v^2} \frac{\partial}{\partial v} \left(\frac{1}{v} \frac{\partial f}{\partial v} + f \right) + \frac{1}{v^3} \frac{\partial}{\partial \mu} (1 - \mu^2) \frac{\partial f}{\partial \mu} \quad (1)$$

where $v^2 = v_{\parallel}^2 + v_{\perp}^2$, $\mu = v_{\parallel}/v$. Velocities are normalized to $v_t = T_e/m_e$, time is normalized to the bulk collisional frequency $\nu = (4\pi e^4 n \ln \Lambda)/(m_e^2 v_t^3)$, where n is the density and $\ln \Lambda$ is the Coulomb logarithm. The diffusion coefficient is $D = (D_{QL})/(v_t^2 \nu)$, where D_{QL} is the quasilinear diffusion coefficient. For the ion charge we have set $Z_i = 1$. We shall now describe the numerical solution of (1) for the time asymptotic state $\frac{\partial f}{\partial \tau} \rightarrow 0$.

We choose a diffusion coefficient of the form:

$$D(v_{\parallel}) = \begin{cases} D_0 & \text{for } v_1 \leq v_{\parallel} \leq v_2 \\ 0 & \text{otherwise} \end{cases} \quad (2)$$

This expression for D follows from an RF power spectrum inside the plasma in which $|E_{\parallel}(k_{\parallel})|^2$ scales like $(1/k_{\parallel})$, where E_{\parallel} is the RF field and k_{\parallel} is the wavenumber along the toroidal magnetic field. This is consistent with a unidirectional spectrum at the plasma edge coupled in by four phased waveguides³ and, in the absence of accurate measurements, is a reasonable assumption. Obviously, we can solve numerically Eq. (1) with any $D(v_{\parallel})$ suggested by the experiments, but the main purpose of this calculation is to provide a check for the 2D theory in the case of D as given by (2).

We find it numerically advantageous to put f in the form:

$$f = \exp(-v^2/2) + f_1(v_{\parallel}, v_{\perp}) \quad (3)$$

There is no requirement for f_1 to be small. Eq. (1) is solved in the region $v_{\min} \leq v, v_{\parallel} \leq v_{\parallel \max}, v_{\perp} \leq v_{\perp \max}$. The mesh is uniformly spaced and typically has 120 points in v_{\parallel} and 60 points in v_{\perp} . The boundary at $v_{\perp} = 0$ is a line of symmetry. In the bulk of the plasma, $v < v_{\min}$, collisions insure that f is a Maxwellian. Therefore we have the condition $f_1(v_{\min}, \mu) = 0$. The $v_{\parallel \max}, v_{\perp \max}$ boundary is sufficiently far out so that $f_1(v_{\parallel \max}, v_{\perp}), f_1(v_{\parallel}, v_{\perp \max})$ are negligible; v_{\max} is chosen large enough not to affect the results for the distribution function at small v . The flux of particles through the boundary $v_{\perp} = 0$ is obviously zero. However, at $v = v_{\min}, v_{\parallel} = v_{\parallel \max}$ and $v_{\perp} = v_{\perp \max}$ there is a finite contribution to the flux. In the time asymptotic state the flow through the computational volume becomes time independent.

The important detail of the solution process resides in the numerical implementation of the algorithm taking the initial f_1 to the time asymptotic state. The usual approach is to simply finite difference the terms in Eq. (1), select a time step Δt small enough for stability, and time integrate the initial distribution to the final configuration. We have achieved a quite significant reduction in the computer time required to get to the asymptotic state by employing two additional techniques.

Firstly, the maximum Δt that can be used in a stable integration scheme – which is proportional to the minimum grid resolution length squared for explicit schemes – is considerably increased by using an alternating-direction-implicit (ADI) procedure for the time advance.¹⁴ Secondly, it is reasonable to assume that during the integration from the initial to the asymptotic state there will be periods for which it is desirable (indeed necessary for stability) to take small Δt 's. Similarly there are also periods during which not much change in f is occurring and much CPU time can be saved by increasing the Δt . What we have implemented for this work is an adaptive Δt

selection procedure which, for reason that will become apparent, we call Aggressive ADI (AADI).

In the procedure we now outline, the guiding principle is that we want to achieve the asymptotic state as fast as possible. This goal is achieved by using as few time steps as possible consistent with stability of the solution. We are not particularly concerned with the details of the time evolution providing we can convince ourselves that the final state is independent of its evolution. We define the residue ϵ as $\epsilon \equiv \left. \frac{\partial f}{\partial \tau} \right|_{max}$, where the subscript *max* refers to the maximum absolute value across the entire v_{\parallel}, v_{\perp} mesh. As long as ϵ decreases, the solution is considered acceptable up to that "time" level and ϵ is saved for future comparison. Δt is gradually increased until ϵ no longer decreases. An increasing ϵ indicates the onset of numerical instability. We follow this last time step, which is on the verge of instability, by a smaller Δt which is intended to allow the solution to stabilize itself. If a reevaluation of ϵ confirms that the solution is again stable (ϵ is again decreasing), the new solution is accepted, and another time step is taken with the same time step size that is near the stability limit *at this time in the integration*. If the small step does not stabilize the solution, a second small step is taken in a final attempt to stabilize the solution. Should it succeed, we are making optimal progress toward the asymptotic limit; should it fail, the last big step and these two small steps are discarded, the solution is restored at the last acceptable configuration, and Δt is reduced substantially before an attempt is made to continue the solution.

This procedure provides for aggressive increases in Δt to the stability limit during periods of inactivity in the time dependence of f_1 . Should the activity increase, a rapid retrenchment is triggered which is very protective of the solution. If a situation is encountered in which the only solution requires an increase in ϵ , this algorithm will fail. The signature of such a mode is that no further time steps are "acceptable" and Δt is reduced to a very small number. This mode is never observed in the present application to Eq. 1. Typically in 2000 steps ϵ can be made smaller than 10^{-10} for this problem.

Numerical results for the case $D_0 = 10$, $v_1 = 4$, $v_2 = 8$ are presented on Figs. 1-3. On Fig. 1 we have a contour plot of the distribution function. One can see the expected flattening of f along v_{\parallel} in the resonance domain. A broadening of the plateau in v_{\perp} leads to a significantly higher perpendicular temperature T_{\perp} , compared with the bulk temperature $T_B = 1$ (in our normalization). On Fig. 2 we show $T_{\perp}(v_{\parallel})$. Note that $T_{\perp} \gg 1$ not only for $v_1 < v_{\parallel} < v_2$ but also for the very energetic particles at $v_{\parallel} > v_2$. This indicates that even outside the resonance region the distribution function significantly deviates from the Maxwellian one. We have also studied the profile of f in the perpendicular direction. In Fig. 3 $f(v_0, v_{\perp})$ with $v_0 = 6$ has been plotted and

a comparison with our analytical results of the next section is made. The values for the currents are found for a wide range of v_1, v_2 and are presented in Table 1. We compare our numerical values with that of the 1D theory¹ and find significantly higher current in all cases. This differs from the conclusion in Ref. 2 that the 2D current, found numerically, is close to the 1D result. There is, however, general agreement on the figure of merit J/P_d between our results and those of Ref. 2. The analytical theory, which we will present now, supports our numerical results. We would like to point out that the contribution to the current comes mostly from the plateau at $v_1 < v_{\parallel} < v_2$. The particles at $v < v_1$ give less than 10% of the total current. However, the energetic particles at $v > v_2$ may contribute as much as 20% of the current.

III. 2D Theoretical Analysis

We shall solve approximately the steady state 2D Fokker-Planck equation in the resonant domain, $v_1 \leq v_{\parallel} \leq v_2$. In (1) we set $\frac{\partial f}{\partial \tau} = 0$ and $D(v_{\parallel})$ as given in (2). The solution for $D_0 \gg 1$ is of the form:

$$f = \varphi(v_{\perp}^2) \exp\left(\frac{1}{D_0} \psi(v_{\parallel}, v_{\perp})\right). \quad (4)$$

$D_0 \gg 1$ is a condition for strong RF diffusion, which is satisfied in most tokamak RF current drive experiments. Using f from (4) substituted into the r.h.s. of (1), and to order one in D_0 we obtain:

$$\frac{\partial^2 \psi}{\partial v_{\parallel}^2} \varphi + \frac{4v_{\parallel}^2}{(v_{\parallel}^2 + x)^{3/2}} (\varphi' + x\varphi'') = 0 \quad (5)$$

where $x \equiv v_{\perp}^2$, $\varphi' = \frac{d\varphi}{dx}$. Terms of order $1/v^2$ have been neglected. If we evaluate the terms to order D_0^{-1} we realize that the approximation is actually $D_0 v_1 \gg 1$.

The figure of merit J/P_d is not very sensitive to the details of the distribution function and we can evaluate it without the explicit knowledge of φ, ψ . The current density due to the particles in the plateau to order one in D_0 and in units of env_t is given by:

$$J = N \int_{v_1}^{v_2} v_{\parallel} dv_{\parallel} \int_0^{\infty} \varphi(x) dx \quad (6)$$

where N is a normalization factor. Similarly, to order one in D_0 and in units of $mn\nu v_t^2$ the density of power dissipated becomes:

$$P_d = N \int_{v_1}^{v_2} dv_{\parallel} \int_0^{\infty} \frac{(v_{\parallel}^2 + x)}{2} \varphi(x) \frac{\partial^2 \psi(v_{\parallel}, x)}{\partial v_{\parallel}^2} dx \quad (7)$$

From (5) and after integrating over v_{\parallel} we obtain:

$$P_d = -N \int_0^{\infty} (\varphi' + x\varphi'')B(x) dx \quad (8)$$

where $B(x) = v_2\sqrt{v_2^2 + x} - v_1\sqrt{v_1^2 + x} - x \ln \frac{v_2 + \sqrt{v_2^2 + x}}{v_1 + \sqrt{v_1^2 + x}}$. An integration by parts leads to:

$$P_d = -N \int_0^{\infty} \varphi \frac{d}{dx}(xB') dx \quad (9)$$

We approximate $B(x)$ in the different intervals of integration:

$$B(x) \simeq v_2^2 - v_1^2 - x \ln \frac{v_2}{v_1} \quad \text{for } x < v_1^2 \quad (10a)$$

$$B(x) \simeq v_2^2 + \frac{x}{2} \left(1 - 2 \ln \frac{2v_2}{\sqrt{x}} \right) \quad \text{for } v_1^2 < x < v_2^2 \quad (10b)$$

$$B(x) \simeq \frac{2}{3\sqrt{x}}(v_2^3 - v_1^3) \quad \text{for } x > v_2^2 \quad (10c)$$

By using the approximate expressions for $B(x)$ one can show that the following inequality is valid:

$$N \ln \frac{v_2}{v_1} \int_0^{\infty} \varphi dx > P_d > N \ln \frac{v_2}{v_1} \int_0^{\infty} \varphi dx - \frac{N}{2}(3 - 2 \ln 2) \int_{v_1^2}^{v_2^2} \varphi dx \quad (11)$$

The second term on the r.h.s. of (11) is a small correction to the first term because only the particles in the resonant plateau in the perpendicular velocity range (v_1, v_2) contribute to the integral. In all cases their number is a small fraction of the total number of particles in the plateau. From (6 and 11) we can estimate the figure of merit.

$$\frac{v_2^2 - v_1^2}{2 \ln \frac{v_2}{v_1}} < \frac{J}{P_d} < \frac{v_2^2 - v_1^2}{2 \ln \frac{v_2}{v_1}} \left(1 - \frac{3 - 2 \ln 2}{2 \ln \frac{v_2}{v_1}} \frac{\int_{v_1^2}^{v_2^2} \varphi dx}{\int_0^{\infty} \varphi dx} \right) \quad (12)$$

With a good accuracy, and most importantly without the details of f which depend on the boundary conditions, we can state that the figure of merit in the 2D theory is 3 times larger than the 1D result:

$$\frac{J}{P_d} = \frac{v_2^2 - v_1^2}{2 \ln \frac{v_2}{v_1}} = 3 \left(\frac{J}{P_d} \right)_{1D} \quad (13)$$

This compares with the factor of 2.5 deduced from the numerical integration results in Ref. 2. The analytical result from (13) are given in Table 1 for a wide range of parameters and they are compared with the figure of merit obtained from our numerical integration of the equations (sec. II) for the same parameters. The agreement is excellent over the whole range and the error is less than 20%.

In order to determine the distribution function (4) we solve Eq. (5) by separating the variables:

$$\frac{\partial^2 \psi}{\partial v_{\parallel}^2} = \frac{4v_{\parallel}^2}{(v_{\parallel}^2 + x)^{3/2}} \eta_0(x) \quad (14)$$

$$\eta_0 \varphi + \varphi' + x \varphi'' = 0. \quad (15)$$

Here η_0 is an arbitrary function of x to be determined from the boundary conditions. An integration of (14) over v_{\parallel} gives:

$$\frac{\partial \psi}{\partial v_{\parallel}} = \eta_1(x) + 4\eta_0(x) \left[\ln(v_{\parallel} + \sqrt{v_{\parallel}^2 + x}) - \frac{v_{\parallel}}{\sqrt{v_{\parallel}^2 + x}} \right] \quad (16)$$

where $\eta_1(x)$ is also a function of x to be found from the boundary conditions.

We require that the distribution function and the parallel flux S_{\parallel} be continuous at $v_{\parallel} = v_1, v_2$. However, $\frac{\partial f}{\partial v_{\parallel}}(v_{\parallel} = v_1, v_2)$ will be discontinuous. We assume that for $v_{\parallel} \rightarrow v_1 (v_{\parallel} < v_1)$ and $v_{\parallel} \rightarrow v_2 (v_{\parallel} > v_2)$, $\frac{\partial f}{\partial v_{\parallel}} = -v_{\parallel} f$. This implies that outside the resonant domain the distribution function retains its Maxwellian character in the parallel direction. We should point out that this assumption is verified by the numerical integration. A change in the slope of f at the boundary points is directly related to the perpendicular temperature in the plateau. A smaller than Maxwellian slope will lead to larger temperatures. Typically, in our model we underestimate the temperature by 20%-50%. The expression for the parallel flux is:

$$S_{\parallel} = -\frac{v_{\parallel}}{v^3} \left(\frac{2x \frac{\partial}{\partial x} + v_{\parallel} \frac{\partial}{\partial v_{\parallel}}}{v^2} + 1 \right) f + \frac{1}{v^3} \left(2v_{\parallel} x \frac{\partial}{\partial x} - x \frac{\partial}{\partial v_{\parallel}} \right) f - D_0 \frac{\partial f}{\partial v_{\parallel}} \quad (17)$$

where $v^2 = v_{\parallel}^2 + x$. For $v^2, D_0 \gg 1$ we find to order one in D_0 and with f given by (4):

where $v^2 = v_{\parallel}^2 + x$. For v^2 , $D_0 \gg 1$ we find to order one in D_0 and with f given by (4):

$$S_{\parallel} = -\frac{v_{\parallel}}{v^3}(\varphi - 2x\varphi') - \varphi \frac{\partial \psi}{\partial v_{\parallel}} \quad (18)$$

The S_{\parallel} outside the resonance plateau ($D = 0$) is given by:

$$S_{\parallel} = -\frac{v_{\parallel}}{v^3}(\varphi - 2x\varphi') + \frac{v_{\parallel}}{v^3} \left(\frac{v_{\parallel}^2}{v^2} + x \right) \varphi \quad (19)$$

To write (19) we have assumed that $f \simeq \varphi$ and $\frac{\partial f}{\partial v_{\parallel}} \simeq -v_{\parallel} \varphi$ for $v \simeq v_1, v_2$. Thus we have incorporated the condition of continuity of the distribution function at the boundary and the assumption of a Maxwellian derivative in the parallel direction.

From (18) and (19) we obtain:

$$\frac{\partial \psi}{\partial v_{\parallel}} = -\frac{v_{\parallel}}{v^3} \left(\frac{v_{\parallel}^2}{v^2} + x \right) \quad \text{for } v_{\parallel} = v_1, v_2 \quad (20)$$

With the expression of $\frac{\partial \psi}{\partial v_{\parallel}}$ from (16) we determine $\eta_0(x)$ and $\eta_1(x)$. The result for $\eta_0(x)$ is substituted in (15) and we are left with a linear second order differential equation to solve. We have integrated this equation numerically and have found that $\varphi(x)$ is very small for $x > v_1^2$. However, for $x < v_1^2$, $\eta_0(x)$ has the simple form:

$$\eta_0(x) = (1+x)\alpha, \quad \alpha \equiv \frac{v_2^2 - v_1^2}{4v_1^2 v_2^2 \ln \frac{v_2}{v_1}} \quad (21)$$

From (15) the equation for φ becomes:

$$\alpha(1+x)\varphi + \varphi' + x\varphi'' = 0 \quad (22)$$

With the substitution

$$\varphi(x) = y(2i\sqrt{\alpha}x) \exp(-i\sqrt{\alpha}x) + c.c. \quad (23)$$

we get Kummer's equation for y and the solution is given in terms of the confluent hypergeometric function M .¹⁵

$$\varphi = A \exp(-i\sqrt{\alpha}x) M\left(\frac{1}{2}(1+i\sqrt{\alpha}), 1; 2i\sqrt{\alpha}x\right) + c.c. \quad (24)$$

where A is a normalization constant. This result is rather complicated and for x such that $\sqrt{\alpha}x < 1$ we find a simple solution:

$$\varphi = A \exp(-\alpha x - \frac{\alpha}{4} x^2). \quad (25)$$

Equation (25) and the expressions for η_0 , η_1 from (16 and 20) determine completely the distribution function in the resonant domain. Note that the assumption of the 1D theory, $\varphi \sim \exp(-x/2)$, does not exhibit the important scaling of α with the position and width of the spectrum. The result for φ in (25) is in good agreement with the cut of f as a function of v_\perp for a fixed v_\parallel as obtained from the numerical integration; see Fig. 3.

The perpendicular temperature in the plateau is given by:

$$T_\perp = \frac{\frac{1}{2} \int_0^\infty x \varphi dx}{\int_0^\infty \varphi dx} = \frac{1}{\sqrt{\pi\alpha}} \quad (26)$$

where T_\perp is normalized to the bulk temperature $T_B = 1$. With α from (21) we find:

$$T_\perp = 2v_1 v_2 \sqrt{\frac{\ln(v_2/v_1)}{\pi(v_2^2 - v_1^2)}} \quad (27)$$

Clearly $T_\perp \gg 1$ and this indicates that the broadening of the distribution function in the perpendicular direction will lead to many more particles in the plateau than estimated by the 1D theory.

The normalization constant for the bulk distribution function is $(1 - \epsilon)/(\sqrt{2\pi})$, where $\epsilon \ll 1$ reflects the fact that some particles have flowed to the resonant plateau. Continuity of f at $x \rightarrow 0$, $v_\parallel \rightarrow v_1$ implies that $A = \frac{1-\epsilon}{\sqrt{2\pi}} \exp(-\frac{v_1^2}{2})$, consistent with our assumption of a Maxwellian character of f along v_\parallel in the domain $D = 0$. It is found from the numerical calculation that the height of the tail of the distribution function is typically two times smaller than estimated by the theory. This is due to the fact that in a boundary layer for $v_\parallel < v_1$ the distribution is non-Maxwellian. This discrepancy explains the almost uniform difference between the analytically and numerically found current, see Table I. If we neglect ϵ , which is at most a few percent, we find for the current in the plateau in units of env_t :

$$J = \frac{\exp(-v_1^2/2)}{2\sqrt{2\pi}} \int_{v_1}^{v_2} dv_\parallel \int_0^\infty dx v_\parallel \varphi(x) \exp(\frac{1}{D_0} \psi(v_\parallel, \sqrt{x})) \quad (28)$$

To order one in D_0 we get:

$$J = \frac{(v_2^2 - v_1^2) \exp(-\frac{v_1^2}{2})}{4\sqrt{2\pi}} \int_0^\infty \varphi(x) dx \quad (29)$$

With φ from (25) the result is:

$$J = \frac{(v_2^2 - v_1^2) \exp(-\frac{v_1^2}{2} + \alpha^2)}{4\sqrt{2}\alpha} [1 + \Phi(\sqrt{\alpha})] \quad (30)$$

where Φ is the error function. In all realistic spectra $\alpha \ll 1$ and (30) gives

$$J = \frac{v_1 v_2}{2} \sqrt{\frac{(v_2^2 - v_1^2) \ln(v_2/v_1)}{2}} \exp(-\frac{v_1^2}{2}) = \frac{\pi}{2} T_{\perp} J_1 \quad (31)$$

where T_{\perp} is given by (27) and J_1 is the current given by the 1D theory. This formula is tested numerically and the results are compared with the 1D theory in Table I. It is clear that for a wide range of parameters our theoretical result (31) predices considerably more current than the 1D theory and typically twice as much as the numerical result. On the other hand the numerical result is 3 to 4 times larger than the 1D theory result.

IV. Summary and Discussion

We have presented a new numerical integration and analytic treatment of the 2D velocity-space Fokker-Planck equation with parallel quasilinear diffusion. This is the basic model equation for describing RF current drive with lower-hybrid waves. Both our numerical and analytic results show that for a given spectrum of wave the values of the current density J are significantly larger, compared with calculations based upon Refs. 1 and 2, and this in our opinion is due to the broadening of the resonant plateau in the direction perpendicular to the toroidal magnetic field. This also entails a larger density of power dissipated. The figure of merit (J/P_d) in the 2D theory is three times larger than the 1D result. Our theoretical analysis of the 2D problem for the regime of strong quasilinear diffusion ($D_0 v_1 \gg 1$) gives approximate analytic expressions for both the current density generated and the enhanced perpendicular temperature inside the parallel velocity range of the spectrum. The limitation of the analytical results lies in an approximate treatment of the boundary layer regions in velocity space at the edges of the spectrum. This notwithstanding, these are the first analytic results from a 2D velocity space analysis and they predict the numerically found results within a factor of two.

Finally, we comment on attempts to explain the recent impressive experimental results^{3,4} on LH current drive. From our results it is clear that a proper description of LH current drive must be based upon a 2D velocity space model of the interaction of collisions and quasilinear diffusion. This should include a proper treatment of the transition regions of the spectrum at both the low and high velocity ends. The later may require a proper relativistic treatment. Such a numerical treatment of the problem

has been carried out recently and shown to predict the observed current generation in Alcator C with only a mild upshift of the applied field spectrum at the plasma edge.¹⁶

Acknowledgments

The authors are grateful to Drs. R. Englade, K. Hizanidis, C. Karney, A. Ram and M. Shoucri for valuable discussion and criticism, and to K. Rugg for help with the computational facilities.

REFERENCES

1. N. J. Fisch, *Phys. Rev. Lett.* **41**, 873 (1978).
2. C.F.F. Karney and N.J. Fisch, *Phys. Fluids* **22**, 1817 (1979).
3. M. Porkolab et al., *Proc. 9th Int. Conf. on Plasma Phys. and Contr. Nucl. Fusion Res.* (Baltimore, U.S.A., 1982), I.A.E.A., Vienna, Austria, **1**, 227 (1983).
4. W. Hooke et al., *Proc. 9th Int. Conf. on Plasma Phys. and Contr. Nucl. Fusion Res.* (Baltimore, U.S.A., 1982), I.A.E.A., Vienna, Austria, **1**, 239 (1983).
5. M. Brambilla, *Nucl. Fusion* **16**, 47 (1976) and **19**, 1343 (1979); V. B. Krapchev and A. Bers, *Nucl. Fusion* **18**, 519 (1978).
6. P. L. Colestock and J. L. Kulp, *I.E.E.E. Trans. Plasma Sci.* **PS-8**, 71 (1980); D. W. Ignat, *Phys. Fluids* **24**, 1110 (1981).
7. P. T. Bonoli and E. Ott, *Phys. Fluids* **25**, 359 (1982); P. L. Andrews and F. W. Perkins, *Phys. Fluids* **26**, 2546 (1983).
8. K. Theilhaber, *Nucl. Fusion*, **22**, 363 (1982).
9. G. Leclert, C. F. F. Karney, A. Bers, and D. J. Kaup, *Phys. Fluids* **22**, 1545 (1979).
10. E. Villalon and A. Bers, *Nucl. Fusion* **20**, 243 (1980).
11. V. S. Chan, C. S. Liu, P. L. Andrews, and F. W. McClain, GA Technologies Report GA-A17450, Feb. 1984; *Proc. of Fourth Varenna/Grenoble Int. Symp. on Heating in Toroidal Plasmas*, Rome Italy, March 21-28, 1984 (in press).
12. S. Von Goeler et al., *Bull. Amer. Phys. Soc.* **27**, 1069 (1982).
13. S. C. Texter et al., *Bull. Amer. Phys. Soc.* **28**, 1162 (1983).
14. R.D. Richtmyer and K.W. Morton, *Difference Methods for Initial-Value Problems*, Wiley (1967).
15. *Handbook of Mathematical Functions*, ed. by M. Abramowitz and I. A. Stegun, Dover, New York (1965).
16. K. Hizanidis, D. W. Hewett and A. Bers, M.I.T.-PFC Report CP/84-4, March 1984; *Proc. Fourth Varenna/Grenoble Int. Symp. on Heating in Toroidal Plasmas*, Rome Italy, March 21-28, 1984 (in press).

FIGURE CAPTIONS

- Fig. 1 Logarithmic contours of a typical steady state distribution function under the influence of an RF spectrum. The spectrum in this example has $D_0 = 10$, $v_1 = 4$, $v_2 = 8$. The contours values are 1, 5, 7 and 9 within each decade starting from 1×10^{-5} on the outside and ending with .5 on the innermost contour. Notice that the normalization of f is 1.0 at $v = 0.0$.
- Fig. 2 The second moment of v_{\perp} integrated for $0 \leq v_{\perp} \leq v_{max}$ is plotted here as a function of v_{\parallel} . This perpendicular temperature T_{\perp} is equal to 1.0 for $f = f_0 = e^{-v^2/2}$ and tends to this value for $v < 3.0$. T_{\perp} is substantially enhanced both in the spectrum region and above.
- Fig. 3 The solid curve is a slice of the distribution function shown in Fig. 1 for constant $v_{\parallel} = 6$. The dashed-dotted line is the expression φ normalized to $f(v_{\parallel} = 6, v_{\perp} = 0)$. Also shown for reference (the dashed line) is the maxwellian $e^{-v_{\perp}^2/2}$ normalized to the same value at $v_{\perp} = 0$.

v_1	v_2	J_1	J_2	J_{num}	J/P_d	J_{num}/P_{num}
3	5	3.6×10^{-2}	1.7×10^{-1}	7.9×10^{-2}	16	15
3	6	6.0×10^{-2}	3.1×10^{-1}	1.4×10^{-1}	20	19
4	6	1.3×10^{-3}	8.1×10^{-3}	3.4×10^{-3}	25	22
3	7	8.9×10^{-2}	4.8×10^{-1}	3.2×10^{-1}	24	22
4	7	2.2×10^{-3}	1.4×10^{-2}	5.5×10^{-3}	30	26
5	7	1.8×10^{-5}	1.3×10^{-4}	8.1×10^{-5}	36	29
3	8	1.2×10^{-1}	6.9×10^{-1}	4.3×10^{-1}	28	27
4	8	3.2×10^{-3}	2.2×10^{-2}	1.1×10^{-2}	35	31
5	8	2.9×10^{-5}	2.3×10^{-4}	9.1×10^{-5}	42	36
6	8	8.5×10^{-8}	7.3×10^{-7}	2.5×10^{-7}	49	41

TABLE I

$v_1(v_2)$ are the low (high) velocity boundaries of the resonant region. From 1D theory $J_1 = \frac{e^{-v_1^2/2}}{\sqrt{2\pi}} \frac{v_2^2 - v_1^2}{2}$, and from 2D theory $J_2 = \frac{e^{-v_1^2/2}}{\sqrt{2}} \frac{v_1 v_2}{2} \sqrt{(v_2^2 - v_1^2) \ln \frac{v_2}{v_1}}$. J_{num} is the result of our numerical integration. $J/P_d = \frac{v_2^2 - v_1^2}{2 \ln \frac{v_2}{v_1}}$ is the approximate result from our 2D theory, and J_{num}/P_{num} is the figure of merit from our numerical integration. J is in units of env_t , P in units of $mv_t^2 \nu n$.

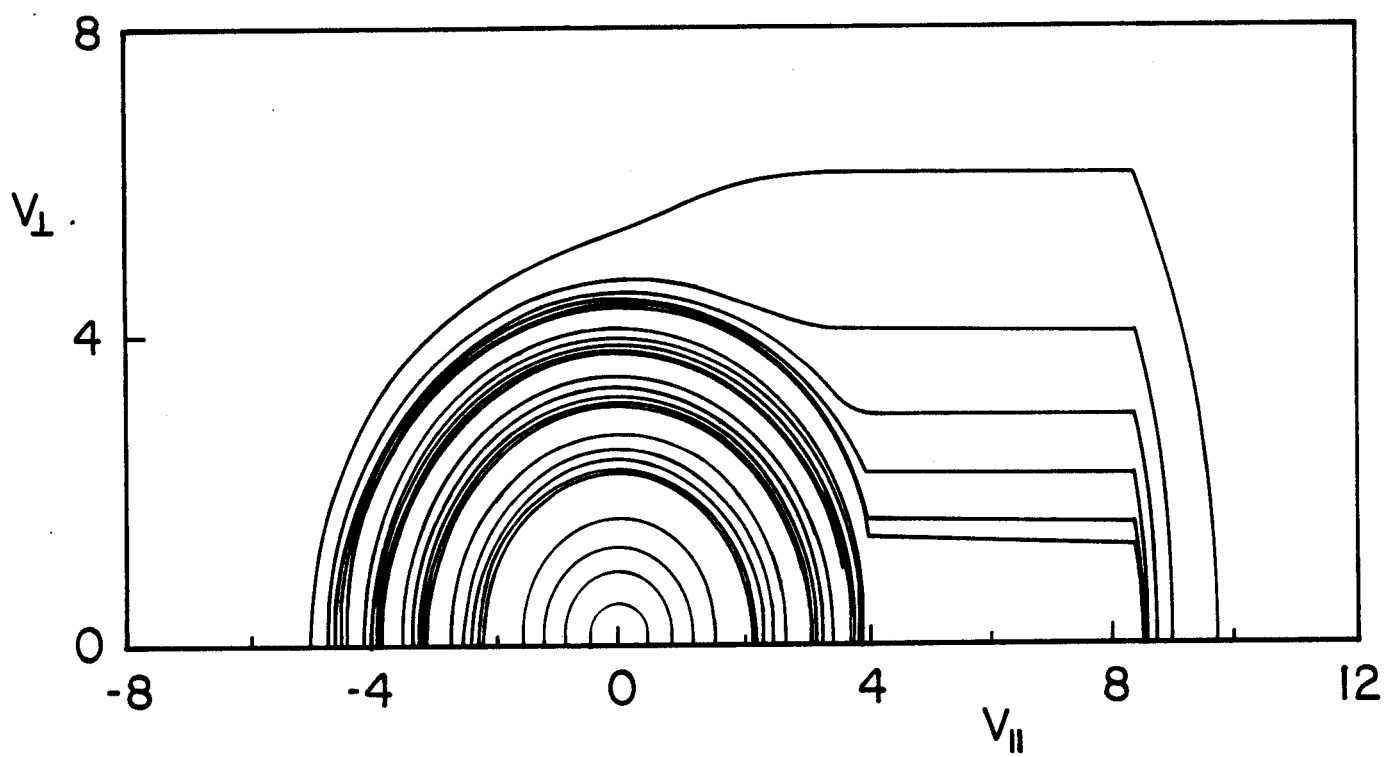


Figure 1

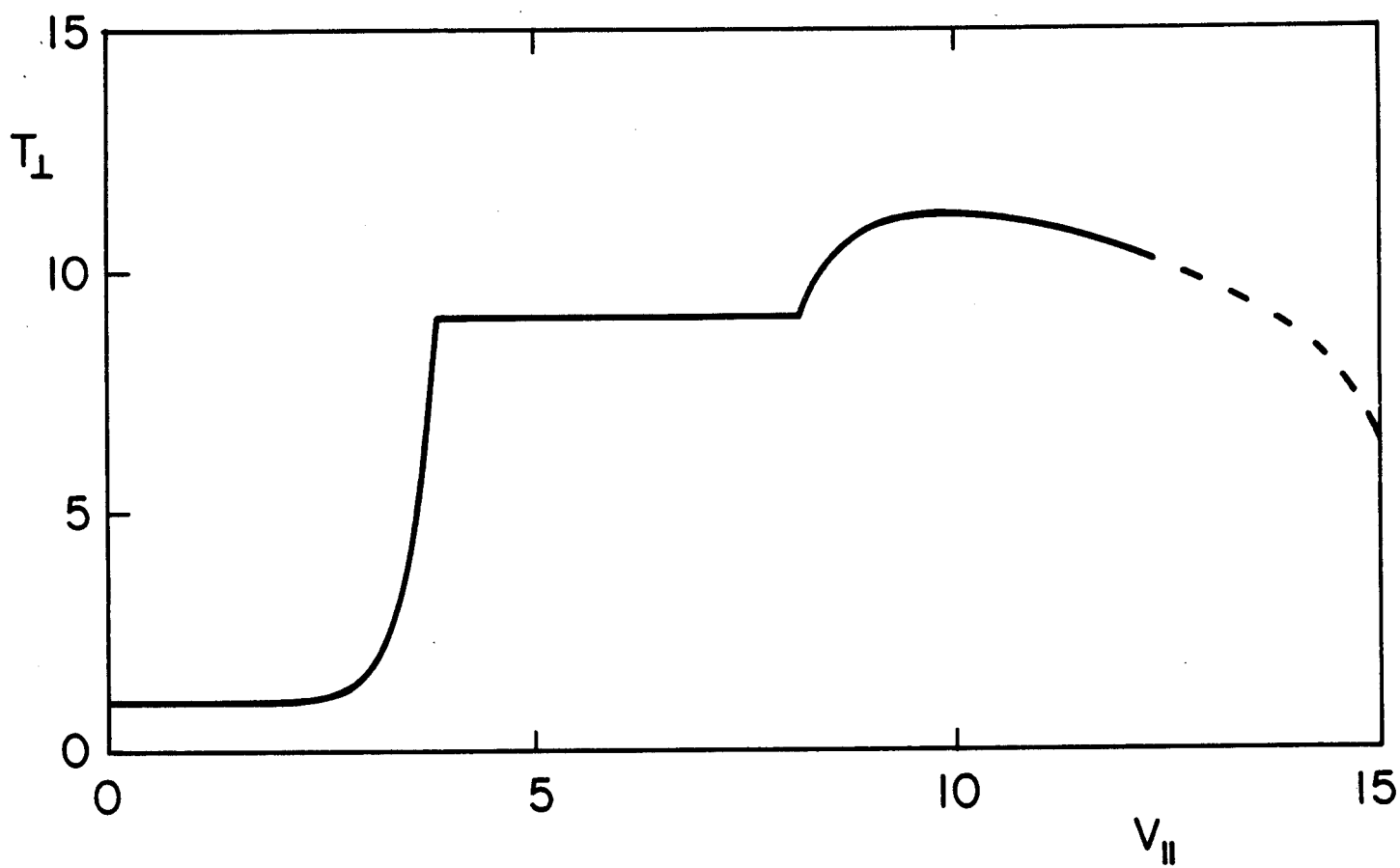


Figure 2

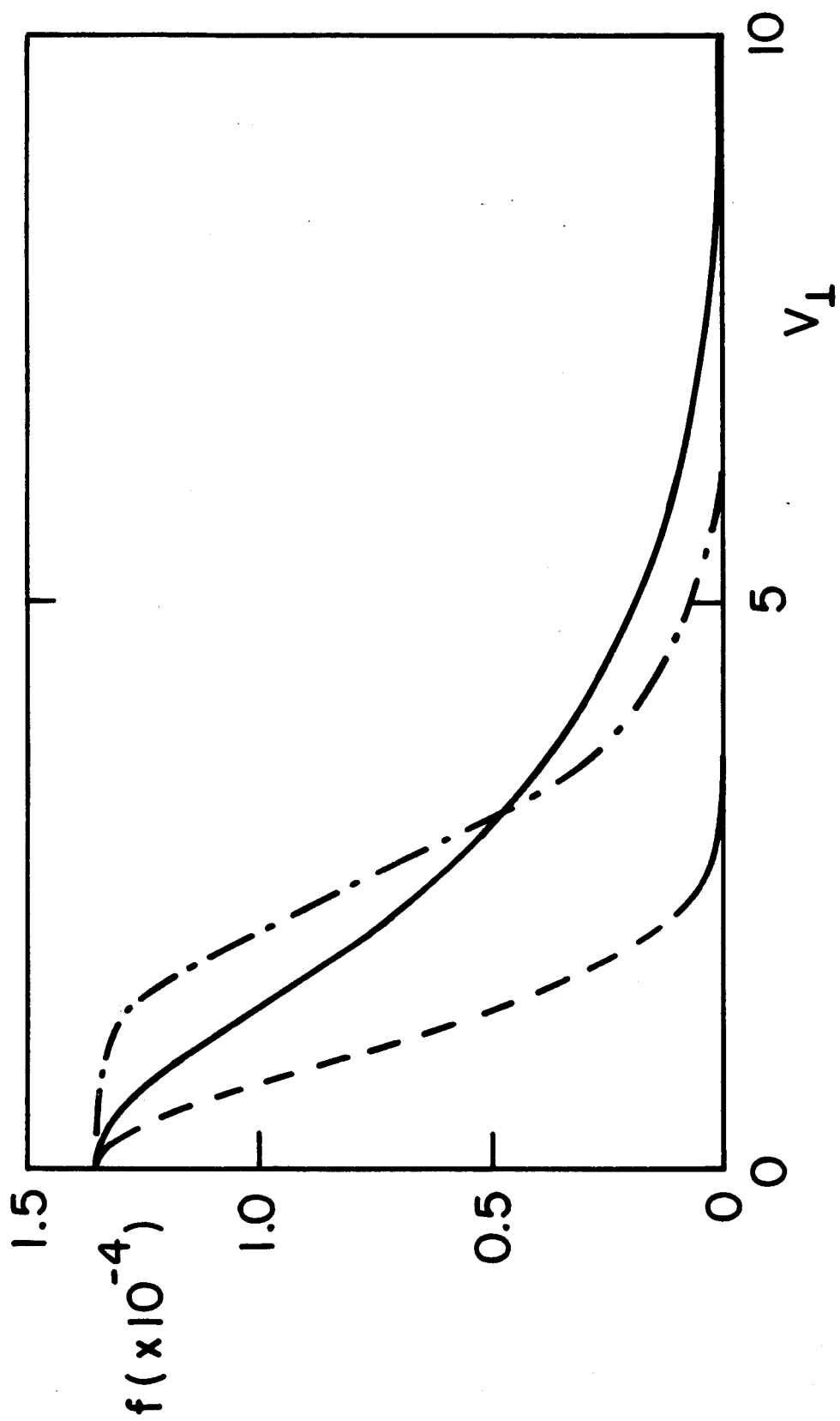


Figure 3